Journal of Hazardous Materials 182 (2010) 252–258

Contents lists available at ScienceDirect

Journal of Hazardous Materials

journal homepage: www.elsevier.com/locate/jhazmat

Catalytic dechlorination of 2,4-dichlorophenol by Pd/Fe bimetallic nanoparticles in the presence of humic acid

Zhen Zhang[a,b], Qiaohui Shen[a], Naman Cissoko[a], Jingjing Wo[a], Xinhua Xu[a,*]

[a] Department of Environmental Engineering, Zhejiang University, Hangzhou 310027, People's Republic of China
[b] School of Bioscience, Taizhou University, Linhai 317000, People's Republic of China

ARTICLE INFO

Article history:
Received 27 January 2010
Received in revised form 4 June 2010
Accepted 6 June 2010
Available online 11 June 2010

Keywords:
Pd/Fe bimetal
Catalytic reduction
2,4-DCP
Humic acid

ABSTRACT

Pd/Fe bimetallic nanoparticles were synthesized for treatment of 2,4-dichlorophenol (2,4-DCP) in the presence of humic acid (HA), in order to understand their applicability for in situ remediation of groundwater. In this case, 2,4-DCP was catalytically dechlorinated to form the final products – phenol (P) via two intermediates, namely *o*-chlorophenol (*o*-CP) and *p*-chlorophenol (*p*-CP). We demonstrated that the carbon mass balances during the dechlorination were in the range of 82–91%, and other carbons were absorbed on the surface of Pd/Fe bimetallic nanoparticles. Our results suggest the dechlorination reaction of 2,4-DCP by Pd/Fe bimetallic nanoparticles in the presence of HA followed pseudo-first-order kinetics. HA competed for reaction sites on the Pd/Fe bimetallic nanoparticles with 2,4-DCP, and thus reduced the efficiency and rate of the dechlorination of 2,4-DCP. Efficiencies of dechlorination and phenol formations increased significantly as the Pd content increased from 0.10 wt.%, 0.15 wt.% to 0.20 wt.%, the removal percentage of 2,4-DCP increased from 70.4%, 98.4% to 99.4% within 300 min, respectively, the nitrate (NO_3^-) content in water also has a significant impact on 2,4-DCP dechlorination efficiency. Our results show that no other intermediates were generated besides Cl^-, *o*-CP, *p*-CP and phenol during the catalytic dechlorination of 2,4-DCP.

1. Introduction

Chlorinated phenols (CPs) constitute an important class of pollutants because of their wide use in the production of wood preservers, pesticides and biocides. Due to their reactive nature, CPs are highly toxic, mutagenic and possibly carcinogenic. Furthermore, they are biorefractory and tend to accumulate in animal tissues. Once released into the environment, CPs will accumulate in the surrounding areas and pose a great health threat to humans and ecosystems over a long period of time [1–3], hence their fate in the environment is of great importance in waste treatment.

Although CPs have been reported to be degraded by bacteria or plants, long reactor residence times are often required to achieve treatment goals [4,5]. Some physical and chemical methods have also been used for the removal of CPs and their derivatives from wastewater including adsorption over activated carbon, air stripping, chemical oxidation, solvent extraction, ultraviolet light and ozone, etc. [1]. However the high cost and low efficiency of these processes limit their applicability.

Permeable reactive barriers (PRBs) packed with zero-valent iron (ZVI, Fe^0) have shown to be an effective technology for the remediation of contaminated groundwaters [6,7]. A rapid and complete dechlorination of chlorinated solvents involving the use of bimetallic Pd/Fe nanoparticles that led to the formation of non-chlorinated hydrocarbons was also reported [8]. Pd/Fe bimetallic nanoparticles, compared to the conventional large particles, have some advantages, these include high specific surface area, high surface reactivity and high efficiency for dechlorination of many chlorinated organic compounds (COCs) due to the presence of palladium, as well as a much lower loading required in the hydrodechlorination process comparing to the common iron or Pd/Fe particles [9,10]. Furthermore, the nanoparticles could remain suspended under conditions of gentle agitation, so it may be possible to inject them into the contaminated soils, sediments and aquifers for in situ remediation of chlorinated organic pollutants [9].

Although nanoscale bimetallic system is effective on the dechlorination of contaminants, the reactivity of the zero-valent metals is highly controlled by the surface characteristics of metals and water chemistry of groundwater. In subsurface environments, natural humic matter is abundant and always plays important roles in both electron transfer and adsorption processes. The inhibition of chlorinated hydrocarbons dechlorination by zero-valent metals in

* Corresponding author. Tel.: +86 571 87951239; fax: +86 571 87952771.
E-mail addresses: xuxinhua@zju.edu.cn, xhxu@hzcnc.com (X. Xu).

0304-3894/$ – see front matter © 2010 Elsevier B.V. All rights reserved.
doi:10.1016/j.jhazmat.2010.06.022

the presence of natural humic matter was reported by Johnson et al. [11]. They suggested that any non-reactive adsorbates that outcompete the contaminants for reactive surface sites would result in a decrease in the degradation rate.

In the present work, we investigated the role of humic acid in the dechlorination of chlorinated hydrocarbons by Pd/Fe bimetallic nanoparticles in order to evaluate the performance of the nanoscale bimetallic systems in the remediation of contaminated groundwater. 2,4-DCP was selected as a model compound due to its abundance in the contaminated groundwater. In addition, other factors such as NO_3^- concentration and Pd loading that may also affect 2,4-DCP reduction were also addressed.

2. Experimental

2.1. Chemicals

Unless noted otherwise, all chemicals including iron sulfate heptahydrate (analytical reagent grade), 2,4-DCP (chemically pure, or CP grade), *o*-CP (CP grade), *p*-CP (CP grade), phenol (CP grade) and other reagents were purchased from the Sinopharm Group Chemical Reagent Co., Ltd., China, and used as received without further purification. Potassium hexachloropalladate (K_2PdCl_6, 99%) and HA were obtained from Sigma–Aldrich. The HA stock solution (500 mg L^{-1}) was prepared by dissolving 0.25 g of HA in 2 mL of a 0.1 M NaOH aqueous solution, followed by sonication, dilution with deionized water to 500 mL, and the pH was adjusted to 7.0. The final HA solution was then filtered through a 0.45 μm pore diameter millipore membrane, HA solutions were stored at 4 °C before use. 2,4-DCP was dissolved in deionized water and stored at 4 °C. Both Fe^0 and Pd/Fe nanoparticles were synthesized immediately before use.

2.2. Synthesis and characterization

Pd/Fe bimetallic nanoparticles were prepared in a 1000 mL three-necked flask under nitrogen gas. Fe nanoparticles were synthesized by dropwise addition of stoichiometric amounts of $NaBH_4$ aqueous solution into a flask containing $FeSO_4{\cdot}7H_2O$ aqueous solution while stirring at 25 °C. The ferrous iron was reduced to zero-valent iron according to the following reaction:

$$Fe(H_2O)_6^{2+} + 2BH_4^- \rightarrow Fe^0 + 2B(OH)_3 + 7H_2 \quad (1)$$

The Fe^0 nanoparticles were then rinsed several times with deionized water. Subsequently, Pd/Fe bimetallic nanoparticles were prepared by reacting the wet Fe^0 nanoparticles with an aqueous solution of potassium hexachloropalladate under stirring according to the following equation:

$$Fe^0 + Pd^{2+} \rightarrow Fe^{2+} + Pd^0 \quad (2)$$

The bimetallic nanoparticles were then rinsed with copious amounts of deionized water to remove excess SO_4^{2-}, Cl^-, Na^+ and K^+ ions.

2.3. Batch experimental procedures

The batch experiments for 2,4-DCP dechlorination in the presence of HA were performed in the same three-necked flask into which Pd/Fe nanoparticles were added. Desired volumes of HA, 2,4-DCP stock solutions and a certain amount of deoxygenated deionized water were added into the flask containing freshly prepared Pd/Fe nanoparticles. The reaction solution was stirred under nitrogen flow. Aliquots of samples were periodically collected with glass syringes and the reaction was quenched by passing through 0.22 μm membrane filters.

2.4. Method of analyses

Fresh metal particles (with a Pd bulk loading of 0.1–0.2%) were visualized under a JEOL JEM 200CX transmission electron microscope (TEM) at 160 kV for morphological measurements. Prior to TEM analysis, the particles were immersed in deionized water and dispersed by a ultrasonator.

Organic compounds such as 2,4-DCP, *p*-CP, *o*-CP and phenol were analyzed by SHIMADZU High Performance Liquid Chromatography. Agilent TC-C18 Column, 150 × 4.6. Mobile phase: MeOH/H_2O (60/40, v/v), flow rate: 1.0 mL min^{-1}, detector: UV at 280 nm, sample size: 20 μL.

Chloride analysis was performed by ion chromatography (792 Basic IC, Metrohm). Column: Metrosep A Supp 4, column size: 4 mm × 250 mm. Analysis condition—eluent: 1.7 mM $NaHCO_3$ + 1.8 mM Na_2CO_3 (with chemical suppression), sample size: 20 μL, flow rate: 1.0 mL min^{-1}, detector: suppressed conductivity detector. Before injection, sample solutions were always filtered through a 0.45-μm membrane filter.

3. Results and discussion

3.1. Characterization of Pd/Fe nanoparticles

Freshly prepared Pd/Fe nanoparticles were black and remained as floccule morphology. Since the size of nanoparticles is smaller than the wavelength of visible light, they serve as a perfect black body that absorbs light. Fig. 1 shows the TEM images of (a) freshly-synthesized Pd/Fe nanoparticles and (b) Pd/Fe nanoparticles in HA solution. The particles are of spherical shape and have a size ranging from 20 nm to 100 nm in diameter. Spherical particles aggregate to form dendrites due to geomagnetic forces between nanoscale particles and small particles, and their surface tension interactions. A mucous layer was adhered onto the surface of Pd/Fe nanoparticles in HA solution, reflecting the possibility of lowering the dechlorination efficiency. A more thicker mucous layer was shown on the surface of the Pd/Fe nanoparticles after 2 h of reaction. More organic components such as HA and 2,4-DCP, as well as metal hydroxides and carbonate passivating layers on the nanoparticles' surface inhibited the particles' active sites, likely leading to lower dechlorination efficiency. These findings are consistent with the observation that HA and contaminations would compete for reactive surface sites [9,12,13].

3.2. Inhibition by humic acid

HA (20 mg L^{-1}) adsorption on Pd/Fe bimetallic nanoparticles was investigated with Pd/Fe nanoparticles dosage of 6.0 g L^{-1} and at an initial pH of 5.7, about 60% adsorption of HA was observed in 1-min period, and more than 95% adsorption of HA occurred after 60 min.

Catalytic dechlorinations of 2,4-DCP over Pd/Fe bimetallic nanoparticles with and without HA are shown in Figs. 2 and 3. 2,4-DCP was first adsorbed by the nanoparticles then reduced to *o*-CP and *p*-CP, and later converted to phenol, phenol was the sole final organic product. No other chlorinated intermediates or final organic products were detected.

The concentration of 2,4-DCP decreased rapidly and the removal percentage reached 98% in 180 min, then reached nearly 100% in 240 min for Pd/Fe nanoparticles in the absence of HA. In contrast, only about 85% and 95% of the removal percentage were obtained in the presence of 10 mg L^{-1} HA during the same reaction periods, respectively. And the concentration of CP remained at low levels during the whole reaction in the absence or presence of HA, the maximum concentration of CP was 0.0225 mM (2.891 mg L^{-1}) in 60 min in the absence of HA, which accounted for 18.6% of the

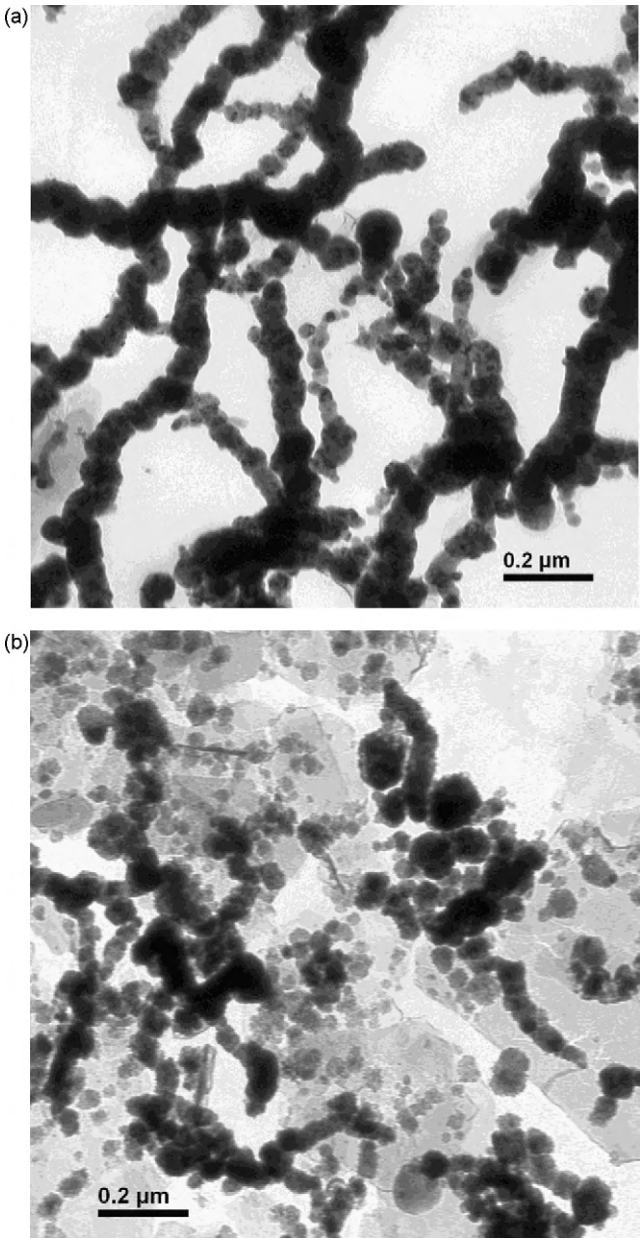

Fig. 1. TEM images of (a) nanoscale Pd/Fe particles in the absence of HA and (b) nanoscale Pd/Fe particles in the presence of HA.

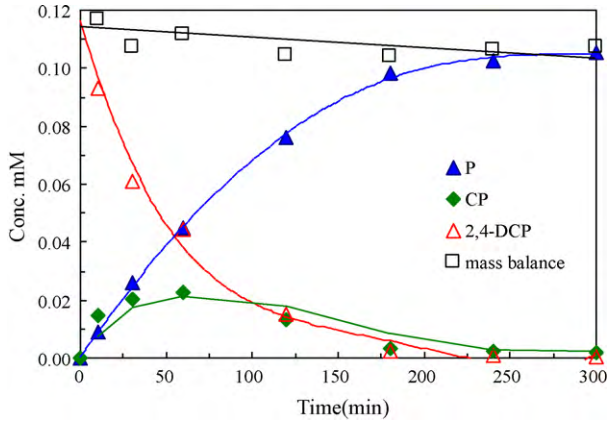

Fig. 2. Dechlorination of 2,4-DCP by Pd/Fe nanoparticles in the absence of HA (T = 30 °C, pH_{in} = 5.7, $C_{2,4\text{-DCP}}$ = 20 mg L^{-1}, $C_{Pd/Fe}$ = 6 g L^{-1}, stirring at 400 rpm, the Pd content was 0.15 wt.%).

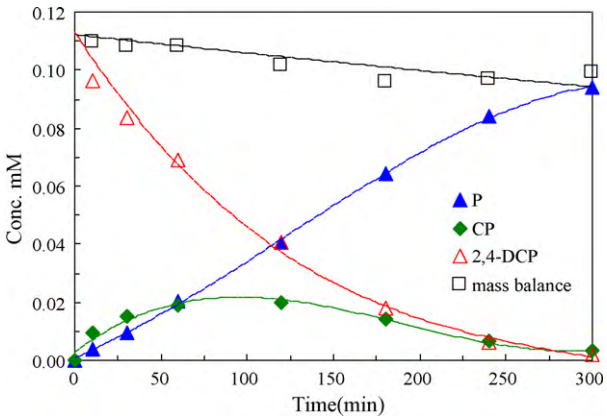

Fig. 3. Dechlorination of 2,4-DCP by Pd/Fe nanoparticles in the presence of HA (T = 30 °C, pH_{in} = 5.7, $C_{2,4\text{-DCP}}$ = 20 mg L^{-1}, C_{HA} = 10 mg L^{-1}, $C_{Pd/Fe}$ = 6 g L^{-1}, stirring at 400 rpm, the Pd content was 0.15 wt.%).

original carbon. The addition of 10 mg L^{-1} HA reduced the removal percentage of 2,4-DCP. Meanwhile the addition of 10 mg L^{-1} HA also lowered the production rate of CP and phenol, which was expressed as the ratio of the total amount of phenol being produced to the theoretical amount of phenol during the complete dechlorination of 2,4-DCP, from 86% in the absence of HA to 78% in two hours, and the maximum concentration of CP was just 0.0199 mM (2.558 mg L^{-1}) in 120 min, which accounted for 16.4% of the original carbon. Phenol and inorganic chlorine were detected as the final products of the dechlorination reaction. Compared to initial concentration (20 mg L^{-1} 2,4-DCP), the carbon mass balances were in the range of 82–91%, so approximately 9–18% carbon mass losses were observed. This indicates that a fraction of organic compounds was absorbed or covered by surface passivating layers due to the precipitation of metal hydroxides on the surface of iron and Pd/Fe particles. This is also evidenced by the fact that the 2,4-DCP concentration dropped rapidly in the first 10 min, but the phenol being generated was much less than the maximum attainable. The non-detected fraction of intermediates may be associated with Pd/Fe nanoparticles, which appear to serve as non-reactive sorption sites for intermediates.

The generation and further catalytic degradation process of *p*- and *o*-CP during the same reaction period with different HA concentrations are presented in Fig. 4. HA concentrations were selected as 0 mg L^{-1}, 10 mg L^{-1} and 20 mg L^{-1} as these concentrations were close to those in groundwater and surface water. The results demonstrated that the generation of *o*-CP was more than that of *p*-CP, although in the further catalytic degradation process, *o*-CP was easily reduced to phenol appreciably than *p*-CP, so the concentration of *o*-CP is much higher than the concentration of *p*-CP during the catalytic dechlorination of 2,4-DCP. The maximum concentrations of *o*-CP were 2.135 mg L^{-1}, 1.687 mg L^{-1} and 1.835 mg L^{-1} with HA 0 mg L^{-1}, 10 mg L^{-1} and 20 mg L^{-1} in 60 min, 120 min and 240 min, respectively, the maximum concentrations of *o*-CP appears delayed as the increase of HA in solution, but for *p*-CP, the maximum concentrations were just 0.756 mg L^{-1}, 0.871 mg L^{-1} and 1.311 mg L^{-1} in 60 min, 120 min and 300 min, respectively, much less than those of *o*-CP. Obviously, the catalytic degradation process slowed down as the increase of HA in solution, the maximum concentrations of *o*-CP and *o*-CP appears delayed, leading to the increase of *o*-CP and *o*-CP concentrations in 300 min when the reaction were terminated, and with the degradation process going on *o*-CP and *p*-CP would be reduced to phenol.

During the catalytic degradation process, most 2,4-DCP are first transformed into *o*-CP and *p*-CP then reduced rapidly to phenol. This was evident from the concentration changes during the

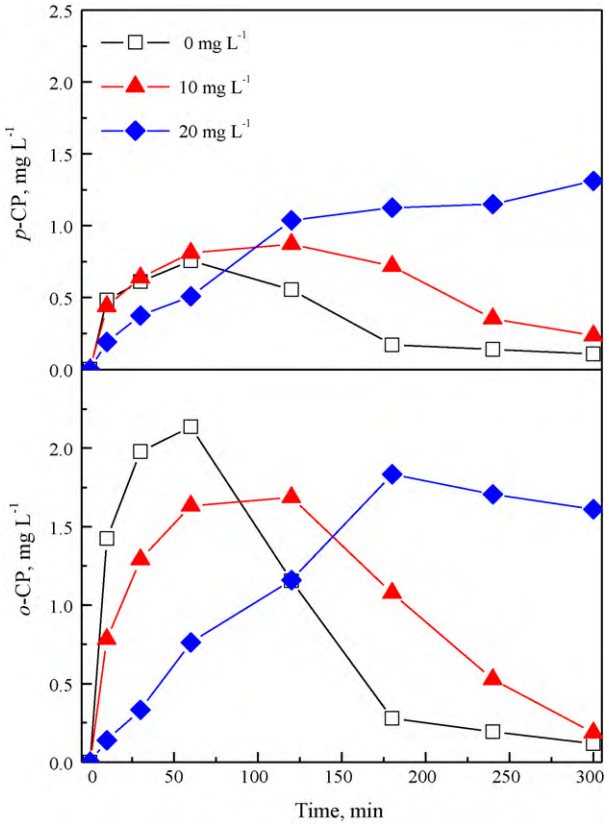

Fig. 4. Effects of HA on the production of *o*-CP and *p*-CP during 2,4-DCP dechlorination by nanoscale Pd/Fe in the presence of HA (T = 30 °C, pH_{in} = 5.7, $C_{2,4\text{-DCP}}$ = 20 mg L^{-1}, $C_{Pd/Fe}$ = 6 g L^{-1}, stirring at 400 rpm, the palladium content was 0.15 wt.%).

reduction of 2,4-DCP, while more and more phenol was produced, the concentration *o*-CP and *p*-CP was initially increased in the prophase reaction, followed by a slow decrease. Phenol and inorganic chlorine were detected as the final products of the reaction. The dependence of the reaction rate constant on the structure of the substrates is not surprising. While the values of ΔG_f^0 of *o*-CP and *p*-CP are −56.8 kJ mol^{-1} and −53.1 kJ mol^{-1} [14], respectively, the variation of the reaction rate constants obtained here is consistent with the previous analysis by Dolfing and Harrison [15]. They showed that the rate constant for the reduction of halogenated aromatics in anaerobic estuarine sediment was proportional to the Gibbs free energy or the activation energy of E_a formation, where E_a is one of the physical chemical parameters of compounds with different molecular structures:

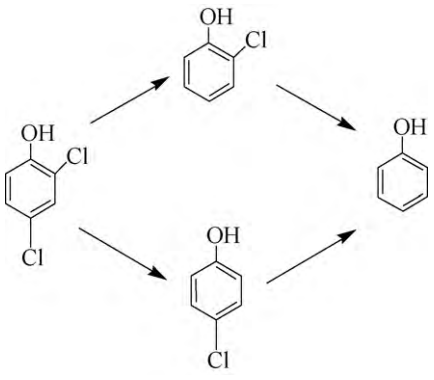

(3)

3.3. Effects of Pd content on 2,4-DCP dechlorination in the presence of humic acid

It has been elucidated that zero-valence iron can promote a hydrogenolysis reaction where a chlorine in the organic chlorinated compounds is replaced by a hydrogen atom. Pd is a well-known excellent catalyst for the hydrogenolysis. The co-existence of Pd and iron in the particles has been proved to be very effective to accelerate the dechlorination. Therefore, the content of Pd loading in the Pd/Fe nanoparticles may be one of the important factors in influencing dechlorination efficiency. As shown in Fig. 5(a), the efficiencies of dechlorination and phenol formations increased significantly as the Pd content was increased from 0.10 wt.%, 0.15 wt.% to 0.20 wt.%. The removal percentage of 2,4-DCP reached from 70.4%, 98.4% to 99.4% within 300 min, respectively. Accordingly, the production yield of phenol increased from 27.4%, 77.6% to 84.7%. The increase in the Pd content from 0.15 wt.% to 0.20 wt.% caused only slight improvement in the dechlorination efficiency. The most likely explanation for this is that the maximum Pd coverage is less than one layer, and in this way, the loss of available catalytic reactive sites due to the overlapping between Pd atoms can be excluded. Nonetheless, the amount of hydrogen gas absorbed by Pd atoms increased with the increasing Pd content [16,17], and so do the efficiencies of dechlorination and phenol formations. The slight improvement of the removal efficiency at Pd content >0.15 wt.% is that the accumulation of excessive hydrogen gas hinders the contact between target pollutant and metal particles and reduces the surface area available for 2,4-DCP dechlorination. This phenomenon is in agreement with previously reported results [10,18]. The optimal Pd content was selected to be about 0.15 wt.% for efficient dechlorination with minimal Pd usage.

The variation of product generation and further catalytic degradation process of *p*- and *o*-CP during the same reaction period under different Pd mass fractions by Pd/Fe bimetallic nanoparticles in the presence of HA is presented in Fig. 5(b). The results demonstrated that more *o*-CP was generated than *p*-CP during the process, although in the further catalytic degradation process, *o*-CP was easily reduced to phenol appreciably than *p*-CP, the maximum concentrations of *o*-CP were 1.693 mg L^{-1}, 1.687 mg L^{-1} and 2.109 mg L^{-1} in 240 min, 120 min and 30 min with a Pd loading of 0.10%, 0.15% and 0.20%, respectively, but for *p*-CP, the maximum concentrations were just 1.567 mg L^{-1}, 0.871 mg L^{-1} and 1.036 mg L^{-1} in 240 min, 120 min and 30 min, respectively. With the increase of Pd loading, the removal efficiency of 2,4-DCP increased proportionally, and the generation of *p*- and *o*-CP also reached a maximum in 30 min for a Pd loading of 0.20%, but it will be 240 min for a Pd loading of 0.10%. Similarly, the catalytic degradation process accelerated for the increasing Pd content, and the maximum concentrations of *o*-CP and *o*-CP appeared advanced, leading to the decrease of *o*-CP and *o*-CP concentrations in 300 min when the reaction was terminated.

3.4. Effects of NO_3^- on 2,4-DCP dechlorination in the presence of humic acid

In subsurface environments, NO_3^- is abundant and plays important roles, NO_3^- pollution of groundwater and surface water has become a serious environmental problem in many parts of the world. Nitrate or nitrite reduction by Fe^0 [19–22] has also received great attention as a potential means for natural attenuation since 1990s. So the concentration effect of NO_3^- on the catalytic dechlorination of 2,4-DCP by Pd/Fe nanoparticles in the presence of humic acid was further examined. Fig. 6(a) illustrates the dechlorination of 2,4-DCP by Pd/Fe nanoparticles at various concentrations of NO_3^- ranging from 0 mg L^{-1} to 50 mg L^{-1} with HA 10 mg L^{-1} to simulate the actual senario in groundwater and surface water. The NO_3^- concentration was increased from 0 mg L^{-1}, 10 mg L^{-1}, 20 mg L^{-1},

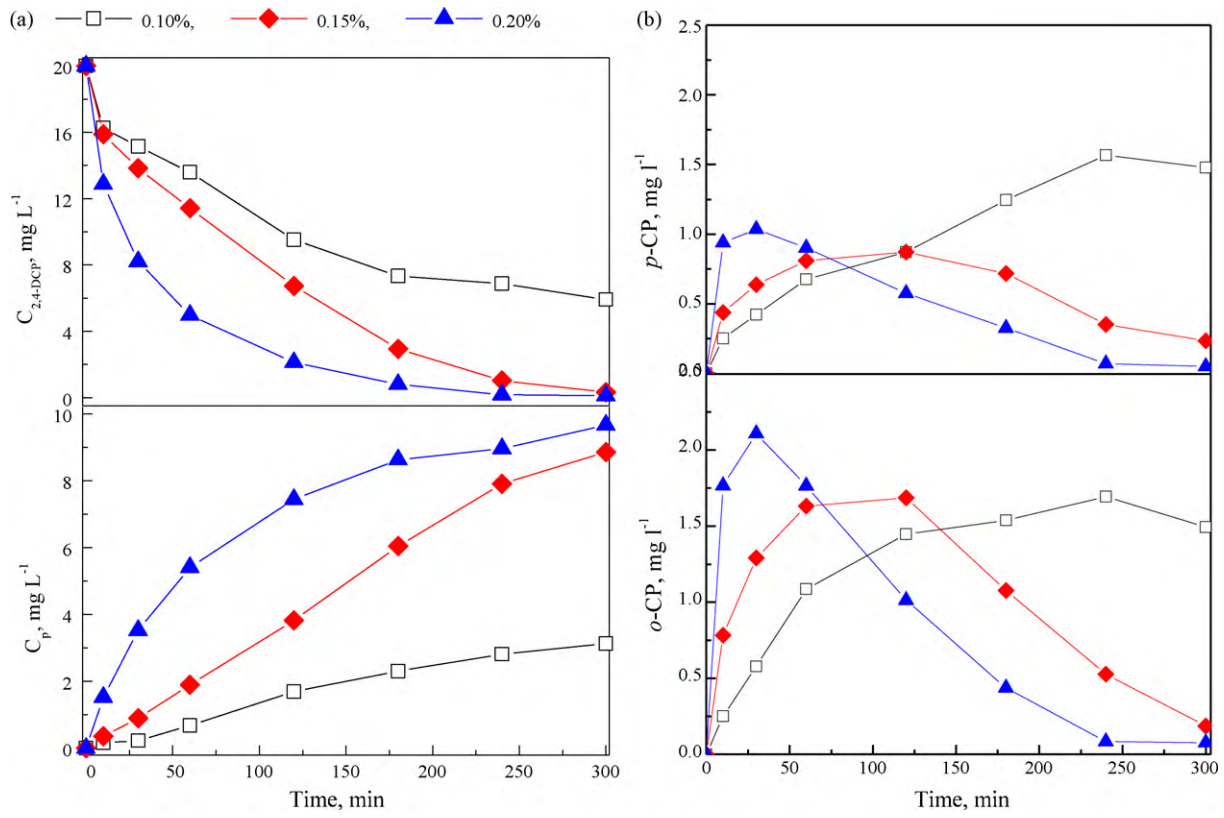

Fig. 5. Effects of the Pd content on catalytic dechlorination of 2,4-DCP by nanoscale Pd/Fe particles in the presence of HA (T = 30 °C, pH_{in} = 5.7, $C_{2,4\text{-DCP}}$ = 20 mg L^{-1}, C_{HA} = 10 mg L^{-1}, $C_{Pd/Fe}$ = 6 g L^{-1}, stirring at 400 rpm). (a) 2,4-DCP and phenol and (b) *o*-CP and *p*-CP.

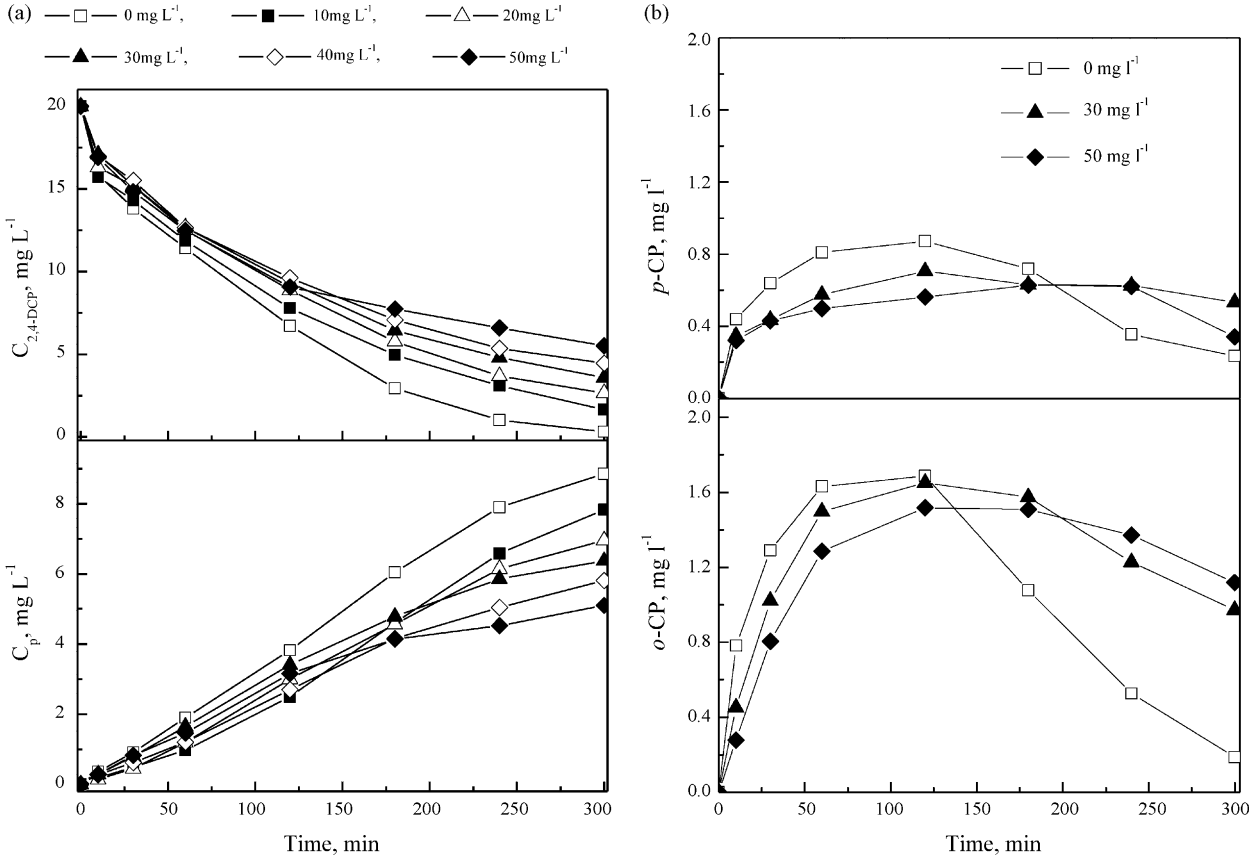

Fig. 6. Effects of NO_3^- on catalytic dechlorination of 2,4-DCP by nanoscale Pd/Fe particles in the presence of HA (T = 30 °C, pH_{in} = 5.7, $C_{2,4\text{-DCP}}$ = 20 mg L^{-1}, C_{HA} = 10 mg L^{-1}, $C_{Pd/Fe}$ = 6 g L^{-1}, stirring at 400 rpm, the palladium content was 0.15 wt.%). (a) 2,4-DCP and phenol and (b) *o*-CP and *p*-CP.

30 mg L^{-1}, 40 mg L^{-1} to 50 mg L^{-1}, which led to a decrease in 2,4-DCP removal percentage from 98.4%, 91.7%, 86.7%, 82.0%, 77.7% to 72.4% in 300 min, and this trend was indeed obvious at much lower NO_3^- concentrations, whereby the same set of NO_3^- concentrations led to a decrease in 2,4-DCP removal percentage from 99.6%, 92.8%, 87.7%, 83.0%, 78.7% to 73.3% in 300 min in the absence of humic acid, respectively. Because HA competed for reaction sites on the Pd/Fe bimetallic nanoparticles with 2,4-DCP, the dechlorination efficiency and rate of 2,4-DCP in the presence of humic acid will less than in the absence of humic acid with the same NO_3^- concentration. Meanwhile the production rates of phenol dropped from 76.8%, 67.9%, 60.4%, 55.3%, 50.4% to 44.2% with a HA concentration of 10 mg L^{-1}, comparing to 85.8%, 77.6%, 67.4%, 61.7%, 56.2% to 52.0% in the absence of humic acid, respectively. And they were found less than those of the dechlorination. The decrease of both 2,4-DCP removal percentages and phenol production rates with the increase of NO_3^- concentrations suggests that the existence of NO_3^- has a significant impact on 2,4-DCP dechlorination efficiency.

The generation and subsequent catalytic degradation of *p*-CP and *o*-CP during the same reaction period at different NO_3^- concentrations are presented in Fig. 6(b). The results demonstrated that more *o*-CP was also formed than *p*-CP during this procedure, and in the subsequent catalytic degradation process, although *o*-CP was easily reduced to phenol appreciably than *p*-CP. The maximum concentrations of *o*-CP were 1.687 mg L^{-1}, 1.652 mg L^{-1} and 1.518 mg L^{-1} at a NO_3^- concentration of 0 mg L^{-1}, 30 mg L^{-1} and 50 mg L^{-1}, respectively, but for *p*-CP, the maximum concentrations were just 0.871 mg L^{-1}, 0.705 mg L^{-1} and 0.627 mg L^{-1}, respectively.

3.5. Kinetics for aqueous phase dechlorination of 2,4-DCP with freshly-synthesized Pd/Fe nanoparticles in the presence of humic acid

The transformations of 2,4-DCP to phenol over Pd/Fe nanoparticles are shown in Figs. 2 and 3. Concentrations in these figures are expressed as molar ratio to initial organic concentration. The products consist of phenol, *p*- and *o*-CP, so it is assumed that 2,4-DCP was hydrodechlorinated according to the following sequence of steps. In the following equations, 2,4-DCP, CP and P are the abbreviated forms of 2,4-dichlorophenol, chlorophenol, and phenol, respectively:

$$2,4\text{-DCP} \xrightarrow{k_1} \text{CP} + \text{Cl}^- \xrightarrow{k_2} \text{P} + 2\text{Cl}^- \quad (4)$$

where CP represents the total molecules of *o*-CP and *p*-CP in the reaction. Previous studies have shown that the degradation reaction of chlorinated solvents by Pd/Fe nanoparticles follows a pseudo-first-order kinetics. The corresponding reaction rate equations for the disappearance of 2,4-DCP, the transient formation of CP (including *o*-CP and *p*-CP) intermediate, and the accumulation of P in the batch system are shown as follows:

$$\frac{-dC_{2,4\text{-DCP}}}{dt} = k_1 C_{2,4\text{-DCP}} \quad (5)$$

$$\frac{dC_{\text{CP}}}{dt} = k_1 C_{2,4\text{-DCP}} - k_2 C_{\text{CP}} \quad (6)$$

$$\frac{dC_{\text{P}}}{dt} = k_2 C_{\text{CP}} \quad (7)$$

The above simultaneous rate equations are solved, leading to the following molar fractions:

$$\alpha_{2,4\text{-DCP}} = e^{-k_1 t} \quad (8)$$

$$\alpha_{\text{CP}} = \frac{k_1}{k_2 - k_1}(e^{-k_1 t} - e^{-k_2 t}) \quad (9)$$

$$\alpha_{\text{P}} = 1 - \alpha_{2,4\text{-DCP}} - \alpha_{\text{CP}} \quad (10)$$

Table 1
k values obtained in the presence of humic acid.

Reaction conditions	$1-\alpha$	k_1	R	k_2	R
Pd ratio in Pd/Fe (wt.%)					
0.10	0.82	0.0039	0.9987	0.005	0.9658
0.15	0.86	0.0086	0.9932	0.018	0.9968
0.20	0.89	0.0230	0.9993	0.022	0.9949
NO_3^- concentration (mg L^{-1})					
0	0.86	0.0086	0.9932	0.018	0.9968
10	0.84	0.0066	0.9986	0.014	0.9950
20	0.87	0.0060	0.9984	0.013	0.9992
30	0.91	0.0056	0.9993	0.013	0.9900
40	0.89	0.0050	0.9982	0.011	0.9930
50	0.88	0.0046	0.9892	0.012	0.9680

where α represents the molar fraction of the subscript compound to the initial concentration of the parent compound (i.e., 2,4-DCP). Since the carbon mass balances were in the range of 82–91%, other carbons were absorbed on the surface of Pd/Fe nanoparticles, the actual concentration of the organic compound in aqueous phase has to be revised. As the production of P was stepwise, the equilibrium time for organic compounds absorbed onto Pd/Fe nanoparticles was little, and the total molar fraction of the organic compounds did not change, the proportion of P in the aqueous phase can be seen as invariable, as a result, Eq. (10) can be revised as follows:

$$\alpha'_{\text{p}} = \alpha_{\text{p}} \times (1 - a) \quad (11)$$

where α represents the molar fraction of the organic compounds which were adsorbed onto Pd/Fe nanoparticles to the initial concentration of the parent compound (i.e., 2,4-DCP). Then *k* values were derived from fitting the experimental data into Eq. (8) according to the non-linear least-square regression. *k* values at different reaction conditions are listed in Table 1. The results show that *k* values for 2,4-DCP dechlorination were increased from 0.0039 min^{-1}, 0.0086 min^{-1} to 0.0230 min^{-1} as the Pd content was increased from 0.10 wt.%, 0.15 wt.% to 0.20 wt.%. In short, *k* values for 2,4-DCP dechlorination dropped from 0.0086 min^{-1}, 0.0066 min^{-1}, 0.0060 min^{-1}, 0.0056 min^{-1}, 0.0050 min^{-1} to 0.0046 min^{-1} with the increase of NO_3^- concentrations from 0 mg L^{-1}, 10 mg L^{-1}, 20 mg L^{-1}, 30 mg L^{-1}, 40 mg L^{-1} to 50 mg L^{-1}, respectively.

4. Conclusion

Our experimental results suggest that HA has an inhibitory effect on the 2,4-DCP dechlorination, and this inhibitory effect was more marked at low HA concentrations. During the dechlorination of chlorinated hydrocarbons, HA could act as an adsorbate to compete reactive sites on the surface of Pd/Fe nanoparticles to decrease the dechlorination rate. The Pd loading in the Pd/Fe nanoparticles is one of the important factors in influencing dechlorination efficiency. And the decrease of both 2,4-DCP removal percentages and phenol production rates with increasing NO_3^- concentrations suggests that the existence of NO_3^- also has a significant impact on 2,4-DCP dechlorination efficiency. It is of great importance to us, as the study helps to better understand the inhibitory mechanisms of HA and other factors on 2,4-DCP dechlorination rates, which will then enable us to optimize reaction conditions in the dechlorination of chlorinated hydrocarbons in order to minimize these inhibitory effects.

Acknowledgements

The authors are grateful for the financial support provided by the Zhejiang Provincial Natural Science Foundation of China (No. R5090033), the National Natural Science Foundation of China (No. 20977086) and the Program for New Century Excellent Talents in University (No. NCET-06-0525).

References

[1] B.W. Zhu, T.T. Lim, J. Feng, Reductive dechlorination of 1,2,4-trichlorobenzene with palladized nanoscale Fe^0 particles supported on chitosan and silica, Chemosphere 65 (2006) 1137–1146.

[2] H. Wang, J.L. Wang, Electrochemical degradation of 4-chlorophenol using a novel Pd/C gas-diffusion electrode, Appl. Catal. B 77 (2007) 58–65.

[3] R.P. Schwarzenbach, E. Molnar-Kubica, W. Giger, S.G. Wakeham, Distribution, residence time, and fluxes of tetrachloroethylene and 1,4-dichlorobenzene in Lake Zurich, Switzerland, Environ. Sci. Technol. 13 (1979) 1367–1373.

[4] Y.T. Wang, P.C. Pai, J.L. Latxhaw, Effects of preozonation of the methanogenic toxicity of 2,5-dichlorophenol, J. Water Pollut. Control Fed. 61 (1989) 320–326.

[5] S.T. Hu, Y.H. Yu, Preozonation of chlorophenolic wastewater for subsequent biological treatment, Ozone Sci. Eng. 16 (1994) 13–28.

[6] R.W. Gillham, S.F. O'Hannesin, Enhanced degradation of halogenated aliphatics by zerovalent iron, Ground Water 32 (1994) 958–967.

[7] H.L. Lien, W.X. Zhang, Nanoscale Pd/Fe bimetallic particles: catalytic effects of palladium on hydrodechlorination, Appl. Catal. B 77 (2007) 110–116.

[8] Y. Fang, S.R. Al-Abed, Dechlorination kinetics of monochlorobiphenyls by Fe/Pd: effects of solvent, temperature, and PCB concentration, Appl. Catal. B 78 (2007) 371–380.

[9] H.L. Lien, W.X. Zhang, Nanoscale iron particles for complete reduction of chlorinated ethenes, Colloids Surf. A 233 (2001) 103–112.

[10] X.Y. Wang, C. Chen, H.L. Liu, J. Ma, Preparation and characterization of PAA/PVDF membrane-immobilized Pd/Fe nanoparticles for dechlorination of trichloroacetic acid, Water Res. 42 (2008) 4656–4664.

[11] T.L. Johnson, W. Fish, Y.A. Gorby, P.G. Tratnyek, Degradation of carbon tetrachloride by iron metal: complexation effects on the oxide surface, J. Contam. Hydrol. 29 (1998) 379–398.

[12] A.P. Davis, V. Bhatnagar, Adsorption of cadmium and humic acid onto hematite, Chemosphere 30 (1995) 243–256.

[13] A.B.M. Giasuddin, S.R. Kanel, H. Choi, Adsorption of humic acid onto nanoscale zerovalent iron and its effect on arsenic removal, Environ. Sci. Technol. 41 (2007) 2022–2027.

[14] Y.H. Liu, F.L. Yang, P.L. Yue, G.H. Chen, Catalytic dechlorination of chlorophenols in water by palladium/iron, Water Res. 35 (2001) 1887–1890.

[15] J. Dolfing, B.K. Harrison, Gibbs free energy of formation of halogenated aromatic compounds and their potential role as electron acceptor in anaerobic environments, Environ. Sci. Technol. 26 (1992) 2213–2216.

[16] Z.L. Liu, X.Y. Ling, X.D. Su, J.Y. Lee, Carbon-supported Pt and PtRu nanoparticles as catalysts for a direct methanol fuel cell, J. Phys. Chem. B 108 (2004) 8234–8240.

[17] C. Grittini, M. Malcomson, Q. Farnando, N. Korte, Rapid dechlorination of polychlorinated biphenyls on the surface of Pd/Fe bimetallic system, Environ. Sci. Technol. 29 (1995) 2898–2900.

[18] J. Xu, Y.J. Wang, Y. Hu, G.S. Luo, Y.Y. Dai, *Candida rugosa* lipase immobilized by a specially designed microstructure in the PVA/PTFE composite membrane, J. Membr. Sci. 281 (2006) 410–416.

[19] S.Y. Ahn, J.H. Oh, K.H. Sohn, Mechanistic aspects of nitrate reduction by Fe(0) in water, J. Korean Chem. Soc. 45 (2001) 395–397.

[20] I.F. Cheng, R. Muftikian, Q. Fernando, Reduction of nitrate to ammonia by zerovalent iron, Chemosphere 35 (1997) 2689–2695.

[21] J.L. Ginner, P.J.J. Alvarez, S.L. Smith, M.M. Scherer, Nitrate and nitrite reduction by Fe^0: influence of mass transport, temperature, and denitrifying microbes, Environ. Eng. Sci. 21 (2004) 219–229.

[22] H.Y. Hu, N. Goto, K. Fujie, Effect of pH on the reduction of nitrite by metallic iron, Water Res. 35 (2001) 2789–2793.